EBioMedicine 28 (2018) 225–233

Contents lists available at ScienceDirect

EBioMedicine

journal homepage: www.ebiomedicine.com

Research Paper

Synthetic High-Density Lipoprotein-Mediated Targeted Delivery of Liver X Receptors Agonist Promotes Atherosclerosis Regression

Yanhong Guo [a,*,1], Wenmin Yuan [b,1], Bilian Yu [a], Rui Kuai [b], Wenting Hu [a], Emily E. Morin [b], Minerva T. Garcia-Barrio [a], Jifeng Zhang [a], James J. Moon [b,c,d], Anna Schwendeman [b,c,**], Y. Eugene Chen [a,*]

[a] Department of Internal Medicine, University of Michigan, Ann Arbor, MI 48109, United States
[b] Department of Pharmaceutical Sciences, University of Michigan, Ann Arbor, MI 48109, United States
[c] Biointerfaces Institute, University of Michigan, Ann Arbor, MI 48109, United States
[d] Department of Biomedical Engineering, University of Michigan, Ann Arbor, MI 48109, United States

ARTICLE INFO

Article history:
Received 17 October 2017
Received in revised form 6 December 2017
Accepted 18 December 2017
Available online 20 December 2017

Keywords:
Atherosclerosis
Liver X receptors
High-density lipoprotein
Reverse cholesterol transport
Macrophage

ABSTRACT

Targeting at enhancing reverse cholesterol transport (RCT) is apromising strategy for treating atherosclerosis via infusion of reconstitute high density lipoprotein (HDL) as cholesterol acceptors or increase of cholesterol efflux by activation of macrophage liver X receptors (LXRs). However, systemic activation of LXRs triggers excessive lipogenesis in the liver and infusion of HDL downregulates cholesterol efflux from macrophages. Here we describe an enlightened strategy using phospholipid reconstituted apoA-I peptide (22A)-derived synthetic HDL (sHDL) to deliver LXR agonists to the atheroma and examine their effect on atherosclerosis regression *in vivo*. A synthetic LXR agonist, T0901317 (T1317) was encapsulated in sHDL nanoparticles (sHDL-T1317). Similar to the T1317 compound, the sHDL-T1317 nanoparticles upregulated the expression of ATP-binding cassette transporters and increased cholesterol efflux in macrophages *in vitro* and *in vivo*. The sHDL nanoparticles accumulated in the atherosclerotic plaques of *ApoE*-deficient mice. Moreover, a 6-week low-dose LXR agonist-sHDL treatment induced atherosclerosis regression while avoiding lipid accumulation in the liver. These findings identify LXR agonist loaded sHDL nanoparticles as a promising therapeutic approach to treat atherosclerosis by targeting RCT in a multifaceted manner: sHDL itself serving as both a drug carrier and cholesterol acceptor and the LXR agonist mediating upregulation of ABC transporters in the aorta.

1. Introduction

Atherosclerosis, characterized by the accumulation of cholesterol and lipids within arterial walls, continues to be a leading cause of morbidity and mortality worldwide. Reverse cholesterol transport (RCT) is an important protective mechanism against atherosclerosis, in which excessive cholesterol from macrophages in the arterial wall is shuttled by high-density lipoprotein (HDL) back to the liver to be ultimately excreted in the feces (Hellerstein and Turner, 2014, von Eckardstein et al., 2001). Cholesterol efflux, the first step of RCT, is the movement of cholesterol from peripheral tissues to HDL and apolipoprotein A-I (ApoA-I), the major protein component of HDL particles. Genetic deficiency for *APOA-I* results in low levels of HDL and premature atherosclerosis (Yokota et al., 2002; Voyiaziakis et al., 1998). In lipid-loaded macrophages, the cholesterol efflux activity is predominately controlled by ATP-binding cassette transporters (ABCA1 and ABCG1) (Adorni et al., 2007). Loss-of-function of *ABCA1* is characterized by impaired RCT and cholesterol accumulation in peripheral tissue macrophages both in humans (known as Tangier disease) and ABCA1-deficent mice (Joyce et al., 2002; Aiello et al., 2002; Wang et al., 2007; Bochem et al., 2013). Overexpression of human APOA-I and macrophage overexpression of ABCA inhibit atherosclerosis by enhanceing reverse cholesterol transport of cholesterol from macrophages to feces (Zhang et al., 2003, Belalcazar et al., 2003, Van Eck et al., 2006). Such findings indicate that modulation of the RCT pathway stands as a prospective strategy to treat atherosclerosis.

One approach involves increasing the cholesterol acceptors, HDL and ApoA-I. However, such approaches have shown no additional reduction of major cardiovascular events(Investigators et al., 2011; Schwartz et al., 2012), perhaps due in part to markedly reduced levels of ABCA1 in advanced atherosclerotic plaques (Albrecht et al., 2004; Tardy et al., 2015). Although statin therapy has shown promising effects in the treatment and prevention of cardiovascular disease, studies have

* Corresponding authors at: Bldg 26, Room 345S, 2800 Plymouth Road, Ann Arbor, MI 48109, United States.
** Correspondence to: A. Schwendeman, Bldg 10, Room 109, 2800 Plymouth Road, Ann Arbor, MI 48109, United States.
E-mail addresses: yanhongg@umich.edu (Y. Guo), annaschw@umich.edu (A. Schwendeman), echenum@umich.edu (Y. Eugene Chen).
[1] Denote equal contribution.

https://doi.org/10.1016/j.ebiom.2017.12.021

shown that statins downregulate ABCA1 expression and ABCA1-mediated efflux in macrophages (Zanotti et al., 2006; Wong et al., 2008). Another approach to enhance RCT is to upregulate the expression of ABC transporters and increase cholesterol effluc in macrophage. Expression of ABCA1 and ABCG1 is mainly regulated by the liver X receptors (LXRα and LXRβ), which are ligand-activated transcription factors that play central roles in the transcriptional control of cholesterol homeostasis and lipid metabolism (Janowski et al., 1996, von Eckardstein et al., 2001). Loss of LXRs accelerates atherosclerotic lesion formation, while synthetic LXR agonists attenuate atherosclerosis and induce atherosclerosis regression through activation of both cholesterol efflux and anti-inflammatory mechanisms (Joseph et al., 2002; Terasaka et al., 2003; Honzumi et al., 2011; Im and Osborne, 2011). However, activation of LXRs induces significant side effects in the liver, including hepatic lipogenesis and hypertriglyceridemia, due to activation of pathways downstream of LXRs, such as sterol regulatory element-binding protein-1 gene (SREBP-1), fatty acid synthase (FASN) and Cytochrome P450 Family 7 Subfamily A Member 1 (CYP7A1) (Schultz et al., 2000; Im and Osborne, 2011). These drawbacks have slowed the progression of LXR agonists into the clinic and halted the development of multiple promising LXR products after Phase I clinical trials. Targeted delivery of an LXR agonist to macrophages in atherosclerotic plaques represents a fundamentally new approach to treat atherosclerosis.

Since HDL particles serve as acceptors of cellular cholesterol efflux and because their hydrophobic core presents a favorable environment for lipophilic drugs, reconstituted HDL has been investigated as a drug delivery system (Duivenvoorden et al., 2014). Recently, we developed a novel nanoparticle-mediated drug delivery system based on synthetic HDL (sHDL), composed of phospholipids and a 22-amino acid ApoA-I-mimetic peptide (22A) (Kuai et al., 2017; Tang et al., 2017). This 22A peptide, used in the synthetic HDL ETC-642 (Di Bartolo et al., 2011), was originally developed as an acute infusion treatment to rapidly mobilize cholesterol from the atheroma, reduce plaque volume and decrease the probability of a second cardiac event. Recent studies have demonstrated that ETC-642 shows anti-inflammatory effect in animal models (Iwata et al., 2011, Di Bartolo et al., 2011).

In this study, we investigated the effects of sHDL nanoparticles (NPs) encapsulating the LXR agonist T0901317 (T1317) on atherosclerosis regression and lipid metabolism. In this nanoparticle-mediated drug-delivery system, sHDL itself acts as both a drug delivery vehicle and cholesterol acceptor, while the encapsulated LXR agonist activates ABC transporters in macrophages, thus targeting simultaneously at least two critical components in the RCT pathway. Furthermore, unlike T1317 compound itself, sHDL-mediated delivery of T1317 does not exhibit some side effects, such as hypertriglyceridemia and the accumulation of triglyceride in the liver.

2. Materials and Methods

2.1. Materials

ApoA-I mimetic peptides 22A with the ends uncapped, PVLDLFRELLNELLEALKQKLK, was synthesized by Genscript Inc. (Piscataway, NJ). The purities of peptide was determined to be over 95% by reserve phase HPLC. Phospholipids 1-palmitoyl-2-oleoyl-sn-glycero-3-phosphocholine (POPC) and 1,2-dimyristoyl-sn-glycero-3-phosphocholine (DMPC) were purchased from NOF America Corporation. T0901317 (T1317, PubChem CID: 447,912, purity >98%, purchased from Cayman Chemical). T1317 was dissolved in DMSO as a stock solution at 10 mg/ml. For animal studies, the stock T1317 solution was diluted with PBS to a final concentration at 0.15 mg/ml and T1317 was administrated at 1.5 mg/kg *via* intraperitoneal (IP) injection immediatedly. The final DMSO concentration in cell culture did not exceed 0.1% throughout the study. All other materials were obtained from commercial sources.

2.2. Preparation of sHDL Nanoparticles

sHDL nanoparticles were prepared using the homogenization method as described (Tang et al., 2017) and the composition of sHDL was 22A peptide, combined with DMPC and POPC (Kuai et al., 2017, Di Bartolo et al., 2011). Lipids and 22A were dissolved in acetic acid, and T1317 compound was dissolved in methanol, those solution were mixed and freeze dried for 24 h. Then the lyophilized powder was hydrated by PBS (pH 7.4) and placed into a water bath to 3 thermal cycles (50 °C for 3 min - iced water bath for 3 min) to form sHDL nanoparticles. The pH of the sHDL solution was adjusted to 7.4 by NaOH. The free peptide and T1317 compound were removed by using 5 ml 7 K MWCO (Sigma). Zeba Spin Desalting columns (ThermoFisher) and the solution was sterile filtered and stored frozen at −20 °C until use. The final concentrations for 22A, DMPC, POPC, and T1317 are 3, 3, 3, and 0.15 mg/ml. The sHDL-DiD was prepared using the same method and the final sample contained 20 μg/ml DiD.

2.3. Analysis of sHDL Nanoparticles

The homogeneity and purity of sHDL and sHDL-T1317 nanoparticle were analyzed by gel permeation chromatography (GPC) with UV detection at 220 nm using Tosoh TSK gel G3000SWx 7.8 mm × 30 cm column (Tosoh Bioscience, King of Prussia, PA) on a Waters Breeze Dual Pump system. The sHDL diameters were determined by dynamic light scattering, using a Zetasizer Nano ZSP (Malvern Instruments, Westborough, MA). The morphology of sHDL nanoparticles were observed by transmission electron microscopy after proper dilution of the original samples with 1% uranyl acetate solution negative staining. The purity, size and release rate of sHDL nanoparticles remained unchanged after 3 freeze-thaw cycles.

2.4. Compound Release Assay

sHDL-T1317 nanoparticles were diluted in release media containing PBS (with 0.02% (w/v) NaN_3, pH 7.4) and the final 22A concentration was 5 mg/ml. To separate the released T1317 from the sHDL-T1317 nanoparticles, 100 mg of biobead Bio-Beads™ SM-2 adsorbent (Bio—Rad Laboratories) was added into 400 μl release media to generate a "sink release condition", in which free T1317 was absorbed on to the adsorbent immediately after release. The retained T1317 in sHDL and 22A peptide in the release media were quantified by HPLC. For the HPLC quantification method, a C18 column (Higgins PROTO 300, 5 μm paticle size, 250 × 4.6 mm) and T1317 and 22A peptide were separated by gradient elution and detected by UV 220 nm absorbance.

2.5. Cellular Cholesterol Efflux Assay

Cholesterol efflux studies were performed, as described previously (Schwendeman et al., 2015; Guo et al., 2015). Murine J774.1 macrophages (ATCC, Manassas, VA) were seeded in 48-well plates for 24 h. Cells were labeled with 1 μCi/ml [1,2-^{3}H]-cholesterol (Perkin Elmer, USA) in DMEM (Life Technology. Inc) containing 0.5% fatty acid-free bovine serum albumin (BSA) and 5 μg/ml ACAT inhibitor Sandoz 58–035 (Sigma) overnight. Then cells were washed twice with PBS and treated with control, sHDL nanoparticles or T1317 compound for 16 h. After collection of the medium, cells were then incubated with DMEM/0.5% BSA containing 50 μg/ml commercial HDL or 10 μg/ml ApoA-I as acceptors for 5 H. Medium was collected and filtered to remove detached cells and efflux was quantified by liquid scintillation and expressed as a percentage of total cell ^{3}H–cholesterol content.

2.6. Quantitative Real-Time PCR

Blood was collected *via* retro-orbital bleeding with EDTA-coated capillaries. Red blood cells were lysed with red blood cell lysis buffer

(Sigma Aldrich). Total RNA was purified from white blood cells and the liver tissue with TRIzol Reagent (Life technologies. Corp.), followed by reverse transcription with a SuperScript III kit (Invitrogen). qPCR was carried out with iQ SYBR Green Supermix (Bio-Rad). Relative abundance of mRNA was normalized to average of 18sRNA and *Ppia*, the housekeeping controls.

2.7. Blood Biochemical Tests

Direct LDL-cholesterol (LDL-c), direct HDL-cholesterol (HDL-c), and enzymatic-colorimetric assays used to determine plasma total cholesterol (TC) and triglycerides (TG) were carried out at the Chemistry Laboratory of the Michigan Diabetes Research and Training Center.

2.8. Atherosclerosis Regression Study

C57BL/6 J mice and *ApoE*-deficient mice were purchased from the Jackson Laboratories and were housed at 22 ± 1 °C in a 12:12-h light-dark cycle. All animal work was performed in accordance with the guidelines set by the University of Michigan Animal Care and Use Committee. Atherosclerosis studies were conducted as described (Guo et al., 2015). Mouse atherosclerotic models were generated by feeding 8-week-old male *ApoE*-deficient mice an atherogenic diet (HFHC, 21% fat, 34% sucrose, and 0.2% cholesterol, Harlan, T.D. 88,137) for 14 weeks. Then the mice were sacrificed (baseline) or switched to chow diet for 6 weeks. Coincident with the switch to chow diet, mice were randomized into 5 groups and received IP injection three times a week (Monday, Wednesday, and Friday) of DMSO, T1317, PBS, sHDL, sHDL-T1317 (sHDL at 30 mg/kg and T1317 at 1.5 mg/kg). Vehicle alone (DMSO or PBS) was used for the control treatment. At the end of the experiment, the mice were anesthetized and subjected to whole-body perfusion to fix the tissues. The entire aorta was microdissected from each mouse. Atherosclerosis was identified by en face oil red O staining, followed by imaging and lesion area quantification using ImageJ software. To quantify the extent of the atherosclerotic lesions in the aortic root, the atherosclerotic lesions in the aortic sinus region was examined at 3 locations, each separated by 80 μm. The largest plaque of the three valve leaflets was adopted for morphological analysis. The lipid-burden plaque areas at the aortic sinus were determined by oil red O staining, followed by imaging and lesion area quantification using ImageJ software.

2.9. Oil Red Staining of Liver Tissue

Mouse livers were fixed with 4% paraformaldehyde and frozen liver sections (10μm) were stained with 5% Oil Red O (Sigma-Aldrich) for 15 min and then stained with haematoxylin. Sections were then examined under light microscopy.

2.10. Determination of Liver Lipid Contents

Liver tissue triglyceride and cholesterol concentrations were measured using Quantification Kits (Biovision, Mountain View, CA). Liver tissues were homogenized in a 5% NP-40 buffer to extract triglycerides. Lipid from liver tissues were extracted with chloroform:isopropyl alcohol:Nonidet P-40 (7:11:0.5). Extracted samples were assayed according to manufacturer's directions. Absorbance was measured on a GloMax-Multi Microplate Multimode Reader.

2.11. Statistical Analysis

Statistical comparisons and analyses between two groups were performed by two-tailed unpaired Student's *t*-test, and among three groups or more, with one-way analysis of variance followed by a Newman-Keuls test. A p value <0.05 was considered statistically significant. Data are presented as mean ± S.E.M.

3. Results

3.1. Design, Preparation and Characterization of sHDL Nanoparticles

Given the limited space for incorporation of compound inside sHDL nanoparticles, we optimized the sHDL formulation and finally utilized DMPC and POPC to synthesize sHDL to achieve the best encapsulation and release rates of T1317 (Fig. 1a). The diameter of the discoid-shaped sHDL nanoparticles was about 11.8 ± 0.3 nm, as determined by dynamic light-scattering and transmission electron microscopy (Fig. 1b, Fig. S1a,b). sHDLT1317 nanoparticles showed similar shape and sized (12.1 ± 0.8 nm) compated to sHDL nanoparticles (Fig. 1b). T1317 is insoluble in water(estimated solubility in water at pH 7.4 is 9.4E-05 mg/ml) and no solid precipitate was found in the solution of sHDL nanoparticles. The average T1317 encapsulation efficiency was 84 ± 2% in three batches of preparation. The *in vitro* T1317 release from sHDL NPs was investigated under physiological conditions (PBS, pH 7.4, 37 °C) and reached 50% and 80% release at 2.4 and 8 h incubation, respectively (Fig. 1c).

3.2. In vitro Efficacy of sHDLT1317 Nanoparticles

To assess the function of sHDLT1317 nanoparticle, we investigated its effects on cholesterol efflux in macrophage. J774A.1 macrophages were incubated with sHDL or sHDLT1317 for 48 h, and cell viability was not markedly changed (Fig. S2a). The ABCA1 transporter is known to primarily promote the cholesterol efflux to lipid-poor or lipid-free apoA-I and thus was able to also promote cholesterol efflux to sHDL NPs (Fig. S2b). sHDL treatment showed a decrease in the expression of ABCA1 and ABCG1 in normal macrophage and cholesterol-loaded foam cells, which may be the subsequence of a decreased cellular cholesterol level after sHDL treatment (Fig. 1d, e, Fig. S2c). As expected, T1317- and sHDLT1317 treatment significantly upregulated the expression of *Abca1* and *Abcg1* in both macrophages and cholesterol-loaded foam cells (Fig. 1d, e). Although T1317 and sHDL induced increased cholesterol efflux compared to controls, sHDLT1317 treatment significantly enhanced total cholesterol efflux to either HDL or ApoA-I acceptors (Fig. 1f, g) in macrophages compared to T1317 or sHDL treatment because that sHDL itself acts as cholesterol acceptor. The cellular cholesterol levels were significantly reduced in T1317 and sHDL-treated cells and further decreased in sHDLT1317-treated cells (Fig. S2c), even after a further incubation with HDL or ApoA-I acceptors (Fig. S2d, e), indicating that targeting at both cholesterol acceptors and ABC transporters results in a synergistic effect on cholesterol efflux.

3.3. Localization of sHDL Nanoparticles in the Atherosclerotic Plaques

To evaluate the ability of sHDL to deliver its cargo (fluorescent dye or T1317 compound) to the atherosclerotic plaques, *ApoE*-deficient mice placed on high fat high cholesterol diet (HFHC) diet were injected with 1,1′-dioctadecyl-3,3,3′,3′-tetramethylindodicarbocyanine (DiD)-loaded sHDL NPs (sHDL-DiD) and imaged using IVIS. We confirmed the accumulation of fluorescent DiD in the aorta 4 h after intraperitoneal injection (IP) of sHDL-DiD (Fig. 2a), suggesting that sHDL could also deliver T1317 to the plaque. Next, we investigated whether sHDL-mediated LXR agonist delivery could regulate LXR target gene expression in atherosclerotic plaques, and the expression of *Abca1* and *Abcg1* was determined in the thoracic aorta. Both of T1317 and sHDLT1317 significantly increased the expression of *Abca1* and *Abcg1* in the aorta (Fig. 2b, c), indicating that sHDL successfully delivered the T1317 to the atheroma and activated the expression of LXR target genes in the atherosclerotic plaques.

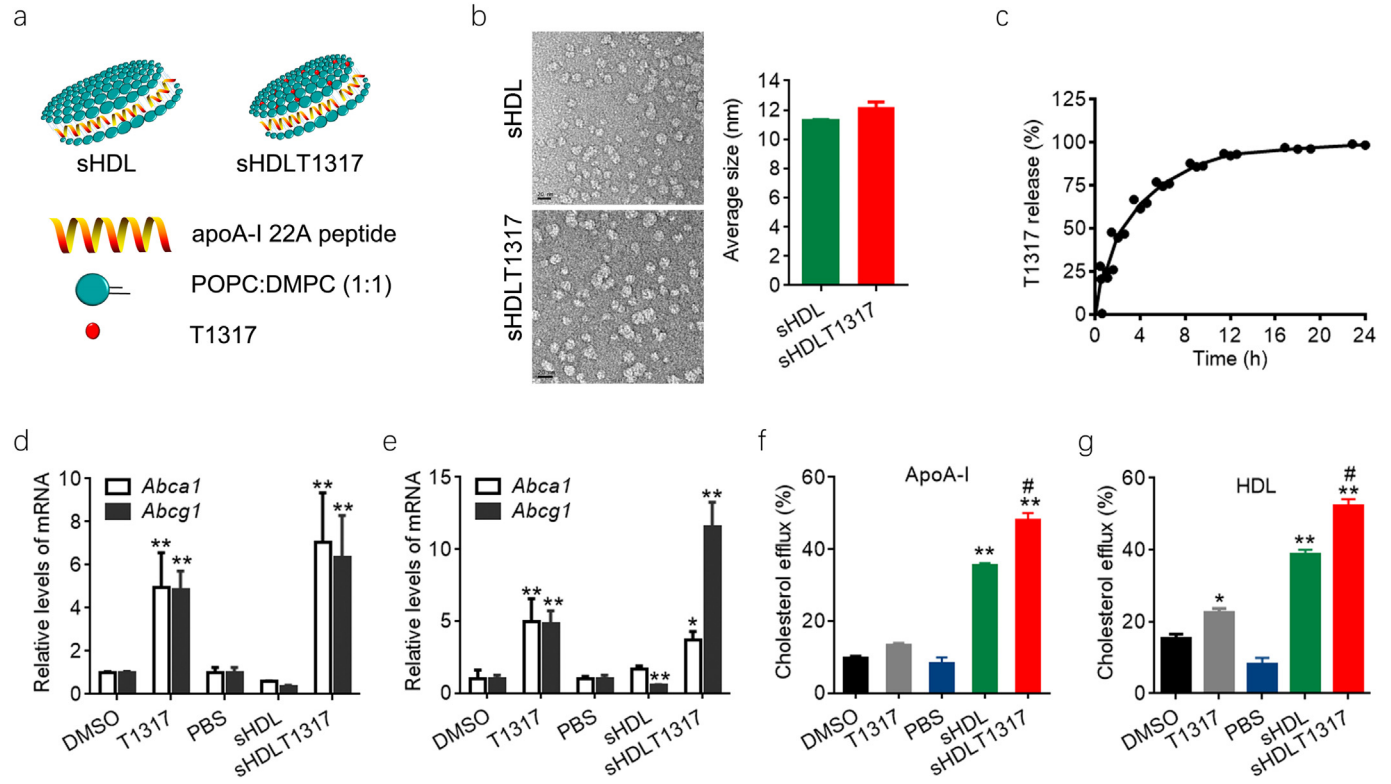

Fig. 1. Schematic representation of the sHDL nanoparticle formulations and efficacy assays. Schematic structure of T1317-encapsulated sHDL NPs (a). Representative TEM images of sHDL and the average size of sHDL and sHDLT1317 (b). The size bar corresponds to 20 μm. (c) *In vitro* release profile of T1317 from sHDL NPs. Quantification of the levels of *Abca1* and *Abcg1* in normal J774A.1 cells (d) and cholesterol loaded J774A.1 foam cells (e). sHDL at 50 μg/ml and T1317 at 0.1 μM. Cholesterol efflux was measured as the percentage of [^{3}H]-cholesterol in the medium after 6 h of incubation with APOA-I at 10 μg/ml (f) or commercial HDL at 50 μg/ml (g). Data are mean ± S.E.M.; $n = 3$–5 per group; $^*P < 0.05$, $^{**}P < 0.01$ compared to control; $\#P < 0.05$, $\#\#P < 0.01$ compared to sHDL.

3.4. Effects of sHDLT1317 on Hepatic Lipogenesis in vivo

The most frequent side effect of LXR agonist administration is fatty liver and increased plasma triglycerides. First, we determined the dosage of T1317 in C57BL/6 mice and found that T1317 induced increased triglyceride levels and activated SREBP1c pathway in the liver even at low dosage (0.5 mg/Kg) (Table 1 and Fig. S3). Then we assessed the functional effects of sHDL NPs on lipid metabolism with the T1317 dosage at 1.5 mg/kg in C57BL/J mice. T1317 compound treatment increased triglyceride levels, induced lipid accumulation in the liver (Fig. 3a, b) and triggered the lipogenesis pathway by activation of *Srebp1, Cyp7a1*, and *Fasn* expression in the liver (Fig. 3c-e). Interestingly, sHDL-

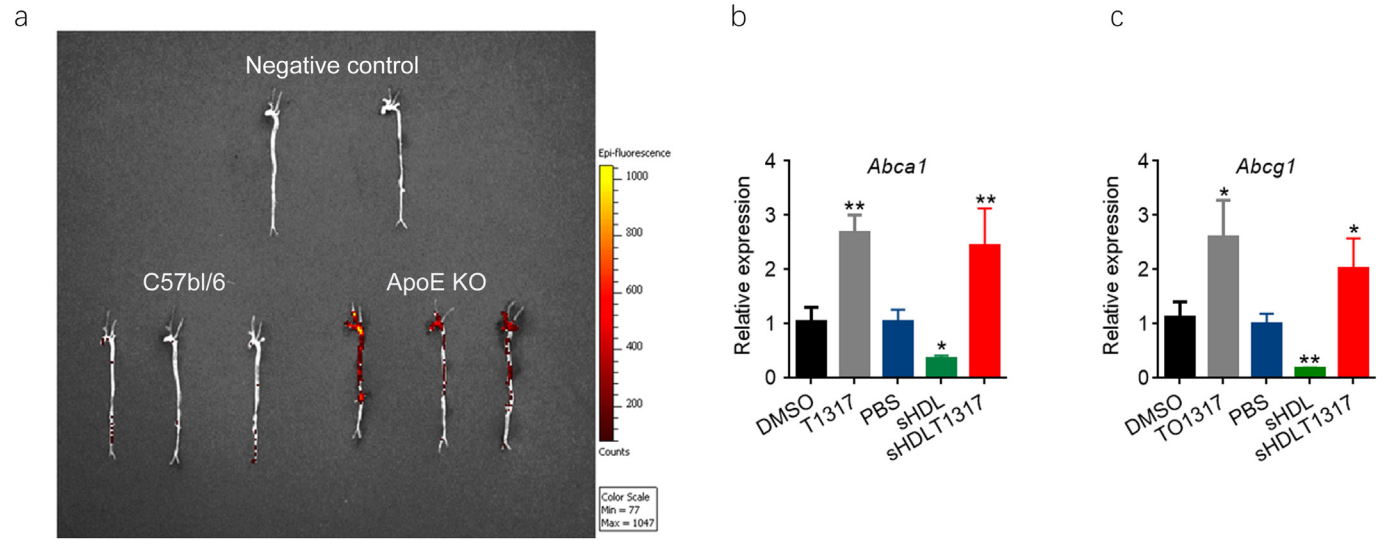

Fig. 2. sHDL nanoparticles delivery cargos into the atherosclerotic plaques. (a) sHDL labeled with DiD (sHDL at 30 mg/kg and DiD at 200 μg/kg) was intraperitoneally injected to *apoE*-deficient mice, which had been placed on HFHC diet for 12 weeks to induce atherosclerotic plaque formation. Four hours later, the aorta were perfused and isolated from the body. Accumulation of DiD in the areas rich in atherosclerotic plaques was observed by IVIS image. DMSO, T1317, PBS, sHDL or sHDLT1317 was injected intraperitoneally in 20-week-old *ApoE*-deficient mice. Four hours later, the aortic arch was collected, RNA was isolated and gene expression of *Abca1* (b) and *Abcg1* (c) was analyzed by quantitative RT-PCR. Data are mean ± S.E.M.; n = 3–5 per group; $^*P < 0.05$, $^{**}P < 0.01$ compared to control; $\#P < 0.05$, $\#\#P < 0.01$ compared to sHDL.

Table 1
Effect of administration of sHDL and T1317 on lipid metabolism and hepatic lipogenesis at different dosage in C57BL/J mice. C57BL/J mice were randomly divided into indicated groups and received once IP injection. Twenty-four hours after injection, the mice were sacrificed.

Group	Total cholesterol (mg/dL)	HDL cholesterol (mg/dL)	Triglycerides
PBS	64.0 ± 2.8	36.3 ± 1.3	79.0 ± 4.3
DMSO	76.9 ± 10.7	45.0 ± 9.2	76.3 ± 8.3
T1317 0.5 mg/kg	110.3 ± 7.2**	46.3 ± 0.8	94.3 ± 12.5*
T1317 1.5 mg/kg	109.3 ± 8.1**	46.3 ± 5.2	101.7 ± 9.6**
T1317 3.0 mg/kg	137 ± 10.4**	55.7 ± 8.9	97.0 ± 4.7**
sHDL	90.0 ± 2.7**	50.7 ± 4.8	72.7 ± 3.3
sHDK-T1317 0.5 mg/kg	79.7 ± 1.9*	44.0 ± 3.6	75.7 ± 3.9
sHDK-T1317 1.5 mg/kg	89.7 ± 2.2*	41.7 ± 1.7	72.3 ± 8.4
sHDK-T1317 3.0 mg/kg	89.0 ± 2.2*	48.3 ± 4.2	72.3 ± 2.5

The total cholesterol, HDL-C and triglyceride levels were measured. Data are mean ± S.E.M.; n = 5 per group; *P < 0.05, **P < 0.01 compared to control.

mediated delivery of T1317 did not increase serum triglyceride levels relative to the sHDL group (Table 1) and sHDLT1317 did not significantly upregulate the expression of LXR-target genes in the liver (Fig. 3c-f). We also observed the effect of sHDL NPs on lipid metabolism after co-administration of sHDL NPs and T1317 by injection at two independent sites (sHDL NPs injected at 30 mg/kg in the left abdomen and T1317 injected in the right abdomen at 1.5 mg/kg). Similar to T1317 compound treatment, this combination resulted in increased triglyceride accumulation in the liver (Fig. 3a, b) and triggered the expression of LXR target genes in the liver (Fig. 3c-e), suggesting that the reduced side effect in the liver by sHDLT1317 is achieved by sHDL-mediated delivery to the atherosclerotic aorta, and not a complementary effect of the combined sHDL and T1317.

3.5. Effects of sHDLT1317 on Atherosclerosis Regression in vivo

We next investigated the biological effect of sHDL-mediated delivery of LXR agonist on atherosclerosis regression *in vivo*. To limit the dominant therapeutic effects of T1317 and sHDL themselves, we used sHDL at 30 mg/kg and a lower dose of T1317 than literature reported dosages (1.5 mg/kg, this dosage significantly activated the expression of *Srebp1*, a LXR target gene which plays critical role in lipogenesis, the liver, Fig. S3). *ApoE*-deficient mice were fed a HFHC diet for 14 weeks to develop atherosclerotic lesions, at which point mice were either sacrificed (baseline) or switched to chow diet for 6 weeks. Coincident with the switch to chow diet, mice were randomly divided into 5 groups, receiving IP injections three times per week with: (i) DMSO vehicle control (DMSO); (ii) T1317 compound at 1.5 mg/kg (T1317); (iii) PBS control (PBS); (iv) sHDL NPs at 30 mg/kg (sHDL); and (v) sHDLT1317 NPs (30 mg/kg sHDL containing 1.5 mg/kg T1317). At the end of the treatment, animals were sacrificed and whole aortas excised for plaque area analysis by oil red O staining (Fig. 4a, b). The baseline *en face* aortic plaque area (22.6 ± 1.8%) increased slightly over the treatment period for the PBS group (24.1 ± 1.4%) and DMSO group (26.4 ± 2.7%). Although we detected the upregulation of *Abca1* and *Abcg1* mRNA expression in white blood cells in T1317-treated group (Fig. 4e, f), T1317 treatment did not signanficantly decrease aortic plaque area (21.6 ± 2.2%) at this lower dosage. sHDL itself showed a slight decrease in aortic plaque area (20.6 ± 1.9%), but the reduction was not found to be statistically significant likely due to the small sample size. The plaque

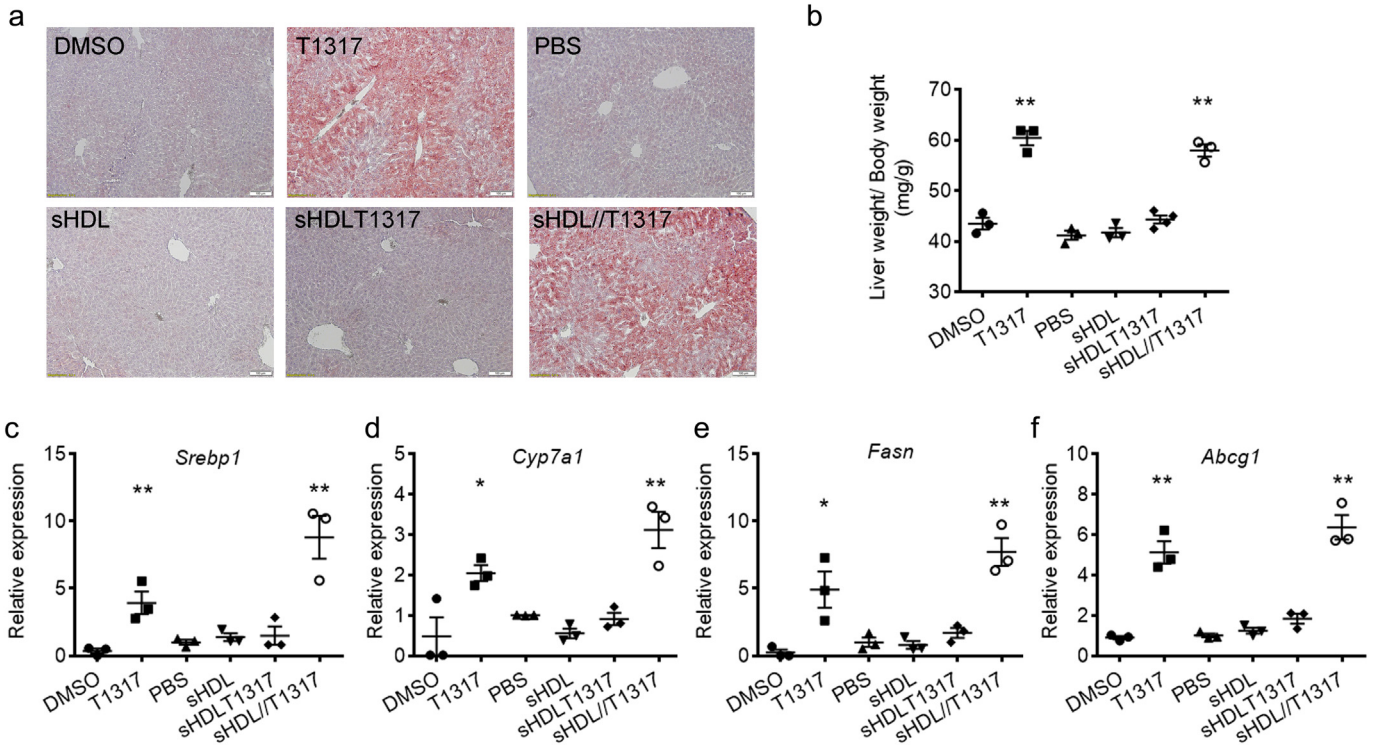

Fig. 3. Effects of combination of sHDL and T1317 on lipid biosynthesis *in vivo*. C57BL/6 mice were randomly divided into 6 groups and received one IP injection per day for continuous four days: (i) DMSO: control; (ii) T1317: T1317 compound in DMSO at 1.5 mg/kg; (iii) PBS: control group; (iv) sHDL: 30 mg/kg of sHDL NPs; (v) sHDLT1317: sHDLT1317 NPs at 30 mg/kg of sHDL and T1317 at 1.5 mg/kg; (vi) sHDL//T1317 (injections at two sites): sHDL NPs at 30 mg/Kg at the left abdomen site and T1317 at 1.5 mg/kg at the right abdomen site. Twenty-four hours after the last injection, the mice were sacrificed. T1317 and sHDL//T1317 treatment resulted in significant lipid accumulation in the liver tissues as assayed by oil red O-stained lesions (a) and increased liver weight over body weight ratio (b). The liver tissues were harvested, RNA was isolated and gene expression of LXR target genes *Srebp1* (c), *Cyp7a1* (d), *Fasn* (e) and *Abcg1* (f) was analyzed by quantitative RT-PCR. Data are mean ± S.E.M.; n = 3–4 per group; *$P < 0.05$, **$P < 0.01$ compared to control.

reduction was statistically significant for sHDLT1317 group (15.0 ± 1.7%) relative to PBS group, and there was a 33.7% reduction in plaque size compared to the baseline. Similar results were obtained from aortic root lesions staining (Fig. 4c, d). Compared to the baseline aortic root plaque area (613.1 ± 45.1 μm^2), DMSO and PBS control groups have no significant change (527 ± 53.2 μm^2 and 579.6 ± 41.6 μm^2 respectively). T1317 and sHDL treatments showed a decrease trend in aortic plaque area (432 ± 43.6 μm^2 and 416.9 ± 32 μm^2 respectively), but the reduction was not found to be statistically significant likely due to the lower dosage. The plaque reduction was statistically significant for sHDLT1317 group (343.2 ± 29.9 μm^2) and there was a 40.8% reduction in aortic root plaque area compared to PBS group.

3.6. Effects of Long-Term Treatment with sHDLT1317 on Lipid Metabolism in vivo

There was no significant difference in total cholesterol, HDL-C and LDL-C levels among the five groups (Fig. 5a-d), however, T1317 administration significantly increased triglyceride levels (432 ± 135 mg/dl compared to DMSO group at 237 ± 65 mg/dl). sHDL NPs slightly

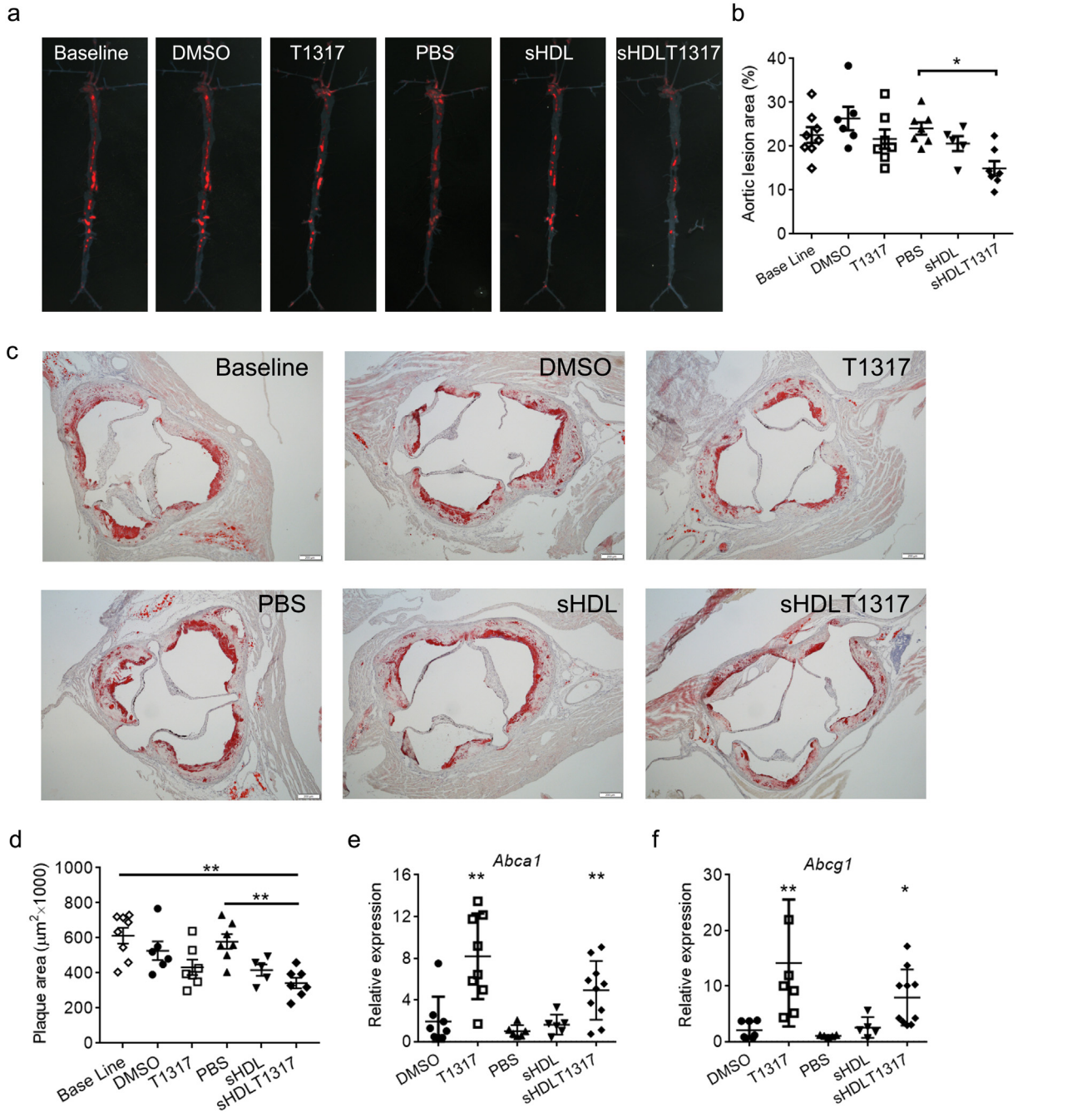

Fig. 4. sHDLT1317 treatment induced atherosclerosis regression by upregulation of ABC transporters. After 14 weeks HFHC diet challenge, *ApoE*$^{-/-}$ mice were randomly divided into six groups and the baseline group animals were sacrificed. The others were switched to chow diet and received IP injection three times per week for 6 weeks: DMSO: control; T1317: T1317 compound in DMSO at 1.5 mg/kg; PBS: control; sHDL: 30 mg/kg; sHDLT1317: 30 mg/kg of sHDL and T1317 at 1.5 mg/kg. sHDLT1317-treated mice exhibited decreased oil red O-stained lesions in the whole aorta (a) and aortic root plaque area (c), corresponding quantitative analyses of the aortas (b) and the aortic root cross-sections (d).RNA was extracted from white blood cells isolated from the mice and gene expression of *Abca1* (e) and *Abcg1* (f) were analyzed by qRT-PCR. Data are mean ± S.E.M.; $n = 5$–9 per group; $^*P < 0.05$, $^{**}P < 0.01$ compared to control.

decreased triglyceride levels (164 ± 57 mg/dl compared to PBS group at 190 ± 35 mg/dl) and sHDLT1317 slightly increased triglyceride levels (274 ± 53 mg/dl), however there were no statistically significant differences among groups (Fig. 5d). T1317 administration also markedly increased triglyceride content in the liver, but this increase was avoided in sHDLT1317-treated animals (Fig. 5e). Liver cholesterol levels for all groups were similar (Fig. 5f). Gene expression analysis of LXR target genes in the liver showed marked increases in *Srebp1*, *Fasn*, *Abca1* and Stearoyl-CoA desaturase-1 (*Scd1*) in the T1317-treated group (Fig. 5g–j), indicating that the T1317 compound itself activated the LXR pathway in white blood cells (Fig. 4e,f) and the liver. However, interestingly, sHDLT1317 treated animals showed very mild increases in the expression of LXR target genes in the liver (Fig. 5g–j) but upregulated *Abca1* mRNA expression in white blood cells (Fig. 5e, f). These findings indicate that sHDL successfully achieved targeted delivery of the inhibitor to the atherosclerotic plaque without induction of the related side effects seen with T1317 administration alone (Fig.6).

4. Discussion

Macrophage accumulation and foam cell formation play a major role in atherosclerotic plaque initiation and progression. Chemical analysis of human atherosclerotic plaques reveals high content and composition of lipids rich in cholesterol and the lipid-rich plaques are strongly associated with majority of acute systemic cardiovascular events among patients with clinically established atherosclerotic disease (Guyton and Klemp, 1996; Sun et al., 2017; Madder et al., 2017). RCT is a protective mechanism through multi-steps to move cholesterol from peripheral tissues such as the vessel macrophages back to liver and then excretion from the body (von Eckardstein et al., 2001). This study reveals that synthetic HDL enables targeted delivery of LXR agonist to induce atherosclerosis regression through enhancing two steps of RCT: 1) increase of the cholesterol acceptor-sHDL and 2) induction of cholesterol efflux in atherosclerotic plaques by LXR agonist. This multifunctional nanocarrier containing LXR agonist selectively activates LXR target genes in atherosclerotic plaques, without inducing significant side effects in the liver.

Although short-term infusions of reconstituted HDL reduce the plaque size and morphology in animal models and in humans, the expression of ABCA1 was down-regulated by infusion of HDL or HDL mimetics (Langmann et al., 1999; Tardy et al., 2015). The down-regulation of ABC transporters could be the result of decreased cholesterol levels in macrophages following HDL mediated cholesterol efflux. However, statins, a first class of lipid-lowering medications, also down-regulate ABCA1 expression and reduce ABCA1-mediated cholesterol efflux in macrophages due to the inhibitory effect on 24(S),25-epoxycholesterol synthesis, a potent oxysterol ligand for LXRα (Qiu and Hill, 2008; Wong et al., 2004). The decreased expression of ABCA1 can attenuate cholesterol efflux, which may partially explain the reason why HDL-cholesterol raising therapies, such as fibrates, niacin, and

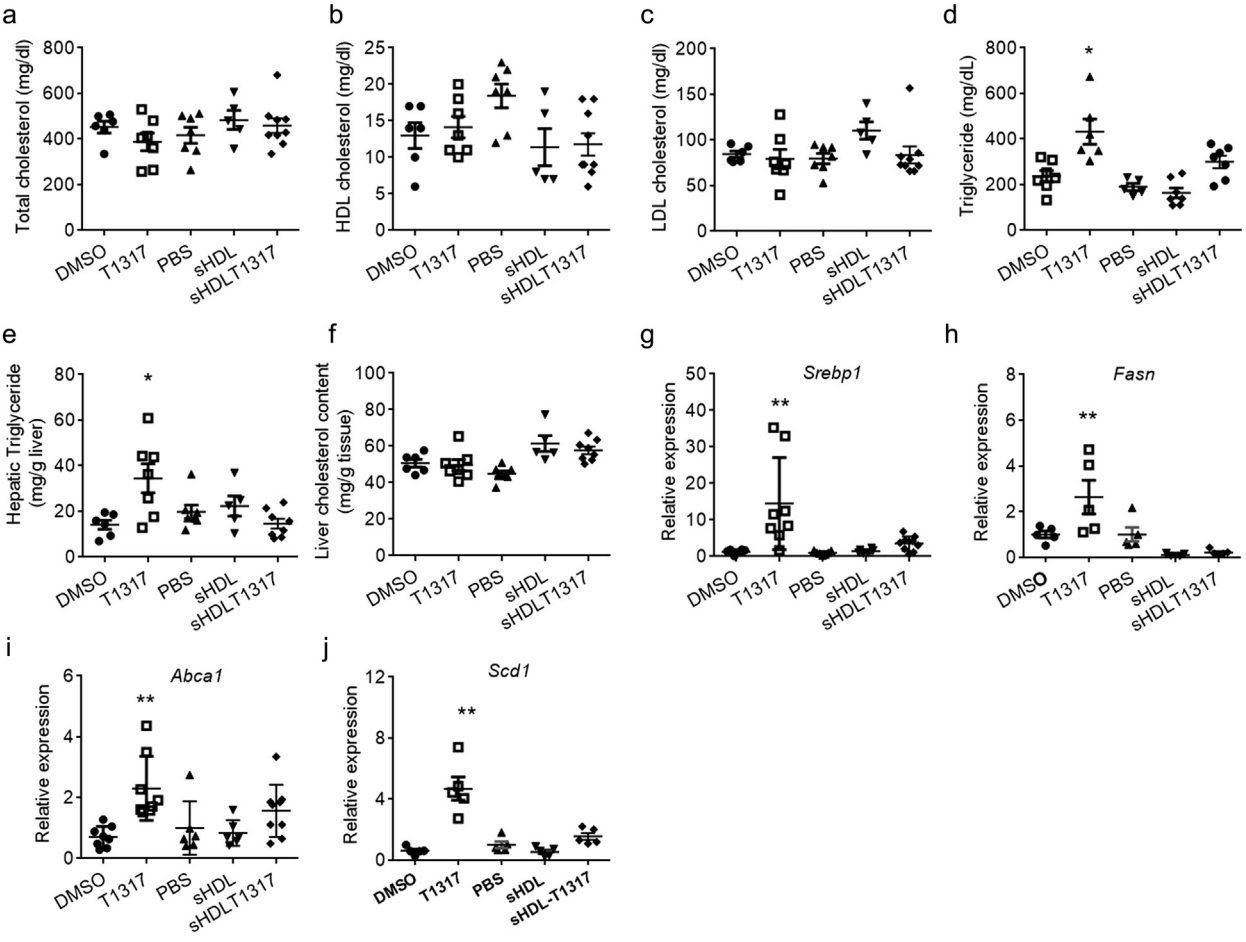

Fig. 5. Long term treatment with sHDLT1317 did not increase triglyceride level and induce hepatic lipogenesis. After 14 weeks HFHC diet challenge, $ApoE^{-/-}$ mice were randomly divided into six groups and the baseline group animals were sacrificed. The others were switched to chow diet and received IP injection three times per week for 6 weeks: DMSO: control; T1317: T1317 compound in DMSO at 1.5 mg/kg; PBS: control; sHDL: 30 mg/kg; sHDLT1317: 30 mg/kg of sHDL and T1317 at 1.5 mg/kg. Plasma total cholesterol (a), HDL cholesterol (b), LDL cholesterol (c) and Triglycerides (d) were measured. The liver triglyceride (e) and cholesterol (f) were extracted and measured. g-j. The liver tissues were harvested from the above animals and gene expression analysis by qRT-PCR of the LXR target genes, *Srebp1* (g), *Fasn* (h), *Abca1* (i) and *Scd1* (j) and. Data are mean ± S.E.M.; n = 5–9 per group; $^{*}P < 0.05$, $^{**}P < 0.01$ compared to control.

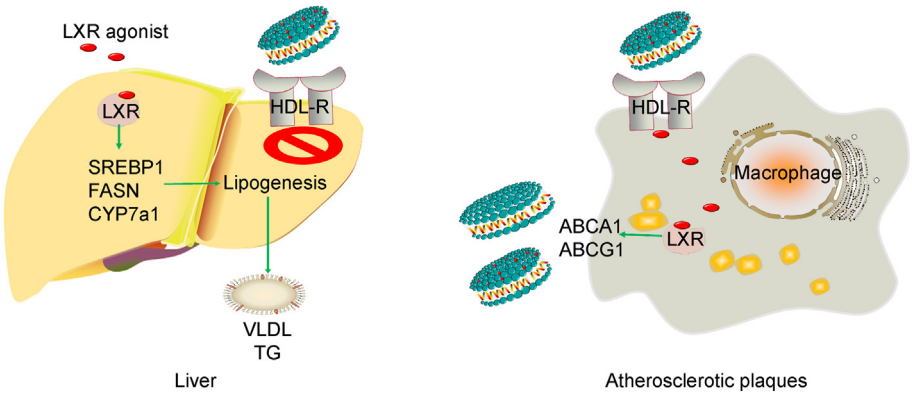

Fig. 6. A working model showing the sHDL NPs-mediated drug delivery system.

cholesteryl ester transfer protein (CETP) inhibitors, have yet to achieve the clinical goal of reducing cardiovascular events (Investigators et al., 2011; Schwartz et al., 2012). It is desirable to manipulate ABC transporters to circumvent the effects of statins and HDL infusions in advanced atherosclerosis.

One of the major aims of the current study was to develop a multifunctional nanocarrier targeting at atherosclerotic plaques. As HDL particles serve as acceptors of cellular cholesterol efflux and the hydrophobic core in the spherical HDL particles has the possibility of incorporating lipophilic drugs, the reconstituted HDL has been investigated as a drug delivery system (Duivenvoorden et al., 2014), but isolation of apolipoproteins from serum limited the therapeutic application. Sanchez-Gaytan developed an HDL-like nanoparticle using poly(lactic-*co*-glycolic acid) (PLGA) and ApoA-I, which also can localize at atherosclerotic plaques (Sanchez-Gaytan et al., 2015). These findings indicate ApoA-I containing-sHDL nanoparticles are a functional carrier targeting at atherosclerotic plaques. In this study, a synthetic ApoA-I mimetic peptide (22-amino acid peptide, 22A) was utilized to formulate sHDL, which overcome the risk of pathogen contamination in making recombinant ApoA-I using bacterial expression system. This 22A peptide, as the mimetic ApoA-I in synthetic HDL-ETC-642, was discovered and developed for the treatment of patients with acute coronary syndromes and has been showed to be safe and well tolerated in phase 1 studies (Iwata et al., 2011). The mean circulation half-life of 22A-sHDL is $T_{1/2}$ = 6.27 h (Tang et al., 2017). Both sHDL and sHDL-T1317 nanoparticles had suitable diameters (average diameter ~12 nm) and T1317 can be delivered to atherosclerotic plaques *in vivo*. Similar to T1317 compound, sHDL-T1317 nanoparticles could upregulate the expression of ABC transporters and increase cholesterol efflux. Although sHDL-DiD could be uptaken by the liver after injection (data not shown), sHDL-T1317 treatment did not triger the expression of LXR target genes in the liver. The uptake of the fluorescent dye (DiD) and the T1317 compound may through different receptor or pathway and the potential underlying mechanisms are under further study. Importantly, sHDL-T1317 nanoparticles did not induce hypertriglyceridemia and hepatic triglyceride accumulation, indicating that sHDL mediated LXR agonist delivery has less lipid metabolism side effects.

LXR has been an attractive drug target for the treatment of atherosclerosis, but remains limited by the hepatic side effects and hypertriglyceridemia. In previous studies, macrophage *Lxr*-deficienciency was associated with significantly increased abundance of atherosclerotic plaques, while macrophage LXRα transgenic mice exhibit a reduction (Tangirala et al., 2002; Teupser et al., 2008). This indicates that the LXR pathway in macrophages plays a central role in the development of atherosclerosis. Unfortunately, it also increases serum and hepatic triglyceride levels *via* activation of the SREBP1c pathway in the liver (Schultz et al., 2000). Targeting plaque macrophages to enhance cholesterol efflux represents an efficient strategy for the treatment and prevention of atherosclerosis. We found that T1317 induced increased triglyceride levels and activated SREBP1c pathway in the liver even at a low dosage (0.5 mg/Kg). Interestingly, sHDL mediated delivery of T1317 did not increase serum triglyceride levels because sHDL-T1317 did not fully activate SREBP1 pathway in the liver meanwhile it activated the expression of ABC transporters in atherosclerotic plaques. The polymeric PLGA nanoparticle containing GW3965, a synthetic LXR agonist, exerts LXR's anti-inflammatory effects and inhibits the development of atherosclerosis without significant hepatic side effects (Zhang et al., 2015). Compared to sHDL nanoparticles, PLGA nanoparticles require surface modification by PEG to prolong their circulation half-life, that may elicit immunologic response and limit repeated injections. Another strategy to targeting at atherosclerotic pleques is using site-specific antibody-drug conjugation that may selectively deliver a LXR agonist to macrophages and inhibit atherosclerosis (Lim et al., 2015; Yu et al., 2017). Compared to those antibodies or particles, sHDL itself offers advantages such as anti-inflammatory effects, binding to ABC transporters, and, most importantly, as cholesterol acceptor. Although the underlying mechanisms of sHDL-mediated atherosclerotic plaque drug delivery need to be further studied, the sHDL delivery system may lead to development of safe and effective therapeutics for atherosclerosis treatment.

In conclusion, we provide an attractive strategy for an sHDL-mediated drug delivery system that targets at atherosclerotic plaque. Synthetic HDL enables targeted delivery of LXR agonist to induce atherosclerosis regression by enhancing at least two steps of RCT: 1) increase of the cholesterol acceptor-sHDL and 2) induction of cholesterol efflux in atherosclerotic plaques by LXR agonist. This multifunctional nanocarrier containing LXR agonist selectively activates LXR target genes in atherosclerotic plaques, while minimizing the adverse side effects in the liver.

Acknowledgements

The authors would like to thank the help and support from Tianqing Zhu and Ricardo Benitez, University of Michigan.

Funding Sources

This study was supported by NIH grants HL068878 and HL134569 (to Y.E.C.), GM113832 and NS091555 (to A.S.), HL134569 (to Y.E.C. and A.S.), American Heart Association grants 15SDG24470155 (to Y.G.), 13SDG17230049 (to A.S.), AHA 16POST27760002 (to W.Y.), T32 GM008353 and T32 HL125242 (E.E.M) and 15PRE25090050 (to R.K).

Conflicts of Interest

None.

Author Contributions

Y.G. and W.Y. conceived the research plan and performed experimental design, did majority of experiments and data analysis. B.Y., R.K., W.H., E.E.M., and J.Z. helped with a portion of experiments and data analysis. M.T.G. and J.J.M. participated in manuscript writing. Y.G., A.S. and Y.E.C. designed this study, performed the study, reviewed and edited the manuscript.

Appendix A. Supplementary data

Supplementary data to this article can be found online at https://doi.org/10.1016/j.ebiom.2017.12.021.

References

Adorni, M.P., Zimetti, F., Billheimer, J.T., Wang, N., Rader, D.J., Phillips, M.C., Rothblat, G.H., 2007. The roles of different pathways in the release of cholesterol from macrophages. J. Lipid Res. 48, 2453–2462.

Aiello, R.J., Brees, D., Bourassa, P.A., Royer, L., Lindsey, S., Coskran, T., Haghpassand, M., Francone, O.L., 2002. Increased atherosclerosis in hyperlipidemic mice with inactivation of ABCA1 in macrophages. Arterioscler. Thromb. Vasc. Biol. 22, 630–637.

Albrecht, C., Soumian, S., Amey, J.S., Sardini, A., Higgins, C.F., Davies, A.H., Gibbs, R.G., 2004. ABCA1 expression in carotid atherosclerotic plaques. Stroke 35, 2801–2806.

Belalcazar, L.M., Merched, A., Carr, B., Oka, K., Chen, K.H., Pastore, L., Beaudet, A., Chan, L., 2003. Long-term stable expression of human apolipoprotein A-I mediated by helper-dependent adenovirus gene transfer inhibits atherosclerosis progression and remodels atherosclerotic plaques in a mouse model of familial hypercholesterolemia. Circulation 107, 2726–2732.

Bochem, A.E., VAN Wijk, D.F., Holleboom, A.G., Duivenvoorden, R., Motazacker, M.M., Dallinga-Thie, G.M., DE Groot, E., Kastelein, J.J., Nederveen, A.J., Hovingh, G.K., Stroes, E.S., 2013. ABCA1 mutation carriers with low high-density lipoprotein cholesterol are characterized by a larger atherosclerotic burden. Eur. Heart J. 34, 286–291.

DI Bartolo, B.A., Nicholls, S.J., Bao, S., Rye, K.A., Heather, A.K., Barter, P.J., Bursill, C., 2011. The apolipoprotein A-I mimetic peptide ETC-642 exhibits anti-inflammatory properties that are comparable to high density lipoproteins. Atherosclerosis 217, 395–400.

Duivenvoorden, R., Tang, J., Cormode, D.P., Mieszawska, A.J., Izquierdo-Garcia, D., Ozcan, C., Otten, M.J., Zaidi, N., Lobatto, M.E., VAN Rijs, S.M., Priem, B., Kuan, E.L., Martel, C., Hewing, B., Sager, H., Nahrendorf, M., Randolph, G.J., Stroes, E.S., Fuster, V., Fisher, E.A., Fayad, Z.A., Mulder, W.J., 2014. A statin-loaded reconstituted high-density lipoprotein nanoparticle inhibits atherosclerotic plaque inflammation. Nat. Commun. 5, 3065.

Guo, Y., Fan, Y., Zhang, J., Lomberk, G.A., Zhou, Z., Sun, L., Mathison, A.J., Garcia-Barrio, M.T., Zhang, J., Zeng, L., LI, L., Pennathur, S., Willer, C.J., Rader, D.J., Urrutia, R., CHEN, Y.E., 2015. Perhexiline activates KLF14 and reduces atherosclerosis by modulating Apo A-I production. J. Clin. Invest. 125, 3819–3830.

Guyton, J.R., Klemp, K.F., 1996. Development of the lipid-rich core in human atherosclerosis. Arterioscler. Thromb. Vasc. Biol. 16, 4–11.

Hellerstein, M., Turner, S., 2014. Reverse cholesterol transport fluxes. Curr. Opin. Lipidol. 25, 40–47.

Honzumi, S., Shima, A., Hiroshima, A., Koieyama, T., Terasaka, N., 2011. Synthetic LXR agonist inhibits the development of atherosclerosis in New Zealand White rabbits. Biochim. Biophys. Acta 1811, 1136–1145.

Im, S.S., Osborne, T.F., 2011. Liver x receptors in atherosclerosis and inflammation. Circ. Res. 108, 996–1001.

Investigators, A.-H., Boden, W.E., Probstfield, J.L., Anderson, T., Chaitman, B.R., Desvignes-Nickens, P., Koprowicz, K., Mcbride, R., Teo, K., Weintraub, W., 2011. Niacin in patients with low HDL cholesterol levels receiving intensive statin therapy. N. Engl. J. Med. 365, 2255–2267.

Iwata, A., Miura, S., Zhang, B., Imaizumi, S., Uehara, Y., Shiomi, M., Saku, K., 2011. Antiatherogenic effects of newly developed apolipoprotein A-I mimetic peptide/phospholipid complexes against aortic plaque burden in Watanabe-heritable hyperlipidemic rabbits. Atherosclerosis 218, 300–307.

Janowski, B.A., Willy, P.J., Devi, T.R., Falck, J.R., Mangelsdorf, D.J., 1996. An oxysterol signalling pathway mediated by the nuclear receptor LXR alpha. Nature 383, 728–731.

Joseph, S.B., Mckilligin, E., Pei, L., Watson, M.A., Collins, A.R., Laffitte, B.A., Chen, M., Noh, G., Goodman, J., Hagger, G.N., Tran, J., Tippin, T.K., Wang, X., Lusis, A.J., Hsueh, W.A., Law, R.E., Collins, J.L., Willson, T.M., Tontonoz, P., 2002. Synthetic LXR ligand inhibits the development of atherosclerosis in mice. Proc. Natl. Acad. Sci. U. S. A. 99, 7604–7609.

Joyce, C.W., Amar, M.J., Lambert, G., Vaisman, B.L., Paigen, B., Najib-Fruchart, J., Hoyt Jr., R.F., Neufeld, E.D., Remaley, A.T., Fredrickson, D.S., Brewer Jr., H.B., Santamarina-Fojo, S., 2002. The ATP binding cassette transporter A1 (ABCA1) modulates the development of aortic atherosclerosis in C57BL/6 and apoE-knockout mice. Proc. Natl. Acad. Sci. U. S. A. 99, 407–412.

Kuai, R., Ochyl, L.J., Bahjat, K.S., Schwendeman, A., Moon, J.J., 2017. Designer vaccine nanodiscs for personalized cancer immunotherapy. Nat. Mater. 16, 489–496.

Langmann, T., Klucken, J., Reil, M., Liebisch, G., Luciani, M.F., Chimini, G., Kaminski, W.E., Schmitz, G., 1999. Molecular cloning of the human ATP-binding cassette transporter 1 (hABC1): evidence for sterol-dependent regulation in macrophages. Biochem. Biophys. Res. Commun. 257, 29–33.

Lim, R.K., Yu, S., Cheng, B., Li, S., Kim, N.J., Cao, Y., Chi, V., Kim, J.Y., Chatterjee, A.K., Schultz, P.G., Tremblay, M.S., Kazane, S.A., 2015. Targeted delivery of LXR agonist using a site-specific antibody-drug conjugate. Bioconjug. Chem. 26, 2216–2222.

Madder, R.D., Vanoosterhout, S., Klungle, D., Mulder, A., Elmore, M., Decker, J.M., Langholz, D., Boyden, T.F., Parker, J., Muller, J.E., 2017. Multimodality Intracoronary Imaging With Near-Infrared Spectroscopy and Intravascular Ultrasound in Asymptomatic Individuals With High Calcium Scores. Circ. Cardiovasc. Imaging 10.

Qiu, G., Hill, J.S., 2008. Atorvastatin inhibits ABCA1 expression and cholesterol efflux in THP-1 macrophages by an LXR-dependent pathway. J. Cardiovasc. Pharmacol. 51, 388–395.

Sanchez-Gaytan, B.L., Fay, F., Lobatto, M.E., Tang, J., Ouimet, M., Kim, Y., VAN DER Staay, S.E., VAN Rijs, S.M., Priem, B., Zhang, L., Fisher, E.A., Moore, K.J., Langer, R., Fayad, Z.A., Mulder, W.J., 2015. HDL-mimetic PLGA nanoparticle to target atherosclerosis plaque macrophages. Bioconjug. Chem. 26, 443–451.

Schultz, J.R., Tu, H., Luk, A., Repa, J.J., Medina, J.C., Li, L., Schwendner, S., Wang, S., Thoolen, M., Mangelsdorf, D.J., Lustig, K.D., Shan, B., 2000. Role of LXRs in control of lipogenesis. Genes Dev. 14, 2831–2838.

Schwartz, G.G., Olsson, A.G., Abt, M., Ballantyne, C.M., Barter, P.J., Brumm, J., Chaitman, B.R., Holme, I.M., Kallend, D., Leiter, L.A., Leitersdorf, E., Mcmurray, J.J., Mundl, H., Nicholls, S.J., Shah, P.K., Tardif, J.C., Wright, R.S., Dal, O.I., 2012. Effects of dalcetrapib in patients with a recent acute coronary syndrome. N. Engl. J. Med. 367, 2089–2099.

Schwendeman, A., Sviridov, D.O., Yuan, W., Guo, Y., Morin, E.E., Yuan, Y., Stonik, J., Freeman, L., Ossoli, A., Thacker, S., Killion, S., Pryor, M., Chen, Y.E., Turner, S., Remaley, A.T., 2015. The effect of phospholipid composition of reconstituted HDL on its cholesterol efflux and anti-inflammatory properties. J. Lipid Res. 56, 1727–1737.

Sun, J., Zhao, X.Q., Balu, N., Neradilek, M.B., Isquith, D.A., Yamada, K., Canton, G., Crouse III, J.R., Anderson, T.J., Huston 3rd, J., O'brien, K., Hippe, D.S., Polissar, N.L., Yuan, C., Hatsukami, T.S., 2017. Carotid plaque lipid content and fibrous cap status predict systemic CV outcomes: the MRI substudy in AIM-HIGH. JACC Cardiovasc. Imaging 10, 241–249.

Tang, J., Li, D., Drake, L., Yuan, W., Deschaine, S., Morin, E.E., Ackermann, R., Olsen, K., Smith, D.E., Schwendeman, A., 2017. Influence of route of administration and lipidation of apolipoprotein A-I peptide on pharmacokinetics and cholesterol mobilization. J. Lipid Res. 58, 124–136.

Tangirala, R.K., Bischoff, E.D., Joseph, S.B., Wagner, B.L., Walczak, R., Laffitte, B.A., Daige, C.L., Thomas, D., Heyman, R.A., Mangelsdorf, D.J., Wang, X., Lusis, A.J., Tontonoz, P., Schulman, I.G., 2002. Identification of macrophage liver X receptors as inhibitors of atherosclerosis. Proc. Natl. Acad. Sci. U. S. A. 99, 11896–11901.

Tardy, C., Goffinet, M., Boubekeur, N., Cholez, G., Ackermann, R., Sy, G., Keyserling, C., Lalwani, N., Paolini, J. F., Dasseux, J. L., Barbaras, R. & Baron, R., 2015. HDL and CER-001 inverse-dose dependent inhibition of atherosclerotic plaque formation in apoE−/− mice: evidence of ABCA1 down-regulation. PLoS One 10, e0137584.

Terasaka, N., Hiroshima, A., Koieyama, T., Ubukata, N., Morikawa, Y., Nakai, D., Inaba, T., 2003. T-0901317, a synthetic liver X receptor ligand, inhibits development of atherosclerosis in LDL receptor-deficient mice. FEBS Lett. 536, 6–11.

Teupser, D., Kretzschmar, D., Tennert, C., Burkhardt, R., Wilfert, W., Fengler, D., Naumann, R., Sippel, A.E., Thiery, J., 2008. Effect of macrophage overexpression of murine liver X receptor-alpha (LXR-alpha) on atherosclerosis in LDL-receptor deficient mice. Arterioscler. Thromb. Vasc. Biol. 28, 2009–2015.

VAN Eck, M., Singaraja, R.R., Ye, D., Hildebrand, R. B., James, E. R., Hayden, M. R. & Van Berkel, T. J., 2006. Macrophage ATP-binding cassette transporter A1 overexpression inhibits atherosclerotic lesion progression in low-density lipoprotein receptor knockout mice. Arterioscler. Thromb. Vasc. Biol. 26, 929–934.

VON Eckardstein, A., Nofer, J.R., Assmann, G., 2001. High density lipoproteins and arteriosclerosis. Role of cholesterol efflux and reverse cholesterol transport. Arterioscler. Thromb. Vasc. Biol. 21, 13–27.

Voyiaziakis, E., Goldberg, I.J., Plump, A.S., Rubin, E.M., Breslow, J.L., Huang, L.S., 1998. Apo A-I deficiency causes both hypertriglyceridemia and increased atherosclerosis in human apo B transgenic mice. J. Lipid Res. 39, 313–321.

Wang, M.D., Franklin, V., Marcel, Y.L., 2007. In vivo reverse cholesterol transport from macrophages lacking ABCA1 expression is impaired. Arterioscler. Thromb. Vasc. Biol. 27, 1837–1842.

Wong, J., Quinn, C.M., Brown, A.J., 2004. Statins inhibit synthesis of an oxysterol ligand for the liver x receptor in human macrophages with consequences for cholesterol flux. Arterioscler. Thromb. Vasc. Biol. 24, 2365–2371.

Wong, J., Quinn, C.M., Gelissen, I.C., Jessup, W., Brown, A.J., 2008. The effect of statins on ABCA1 and ABCG1 expression in human macrophages is influenced by cellular cholesterol levels and extent of differentiation. Atherosclerosis 196, 180–189.

Yokota, H., Hashimoto, Y., Okubo, S., Yumoto, M., Mashige, F., Kawamura, M., Kotani, K., Usuki, Y., Shimada, S., Kitamura, K., Nakahara, K., 2002. Apolipoprotein A-I deficiency with accumulated risk for CHD but no symptoms of CHD. Atherosclerosis 162, 399–407.

Yu, M., Amengual, J., Menon, A., Kamaly, N., Zhou, F., Xu, X., Saw, P.E., Lee, S.J., Si, K., Ortega, C.A., Choi, W.I., Lee, I.H., Bdour, Y., Shi, J., Mahmoudi, M., Jon, S., Fisher, E.A., Farokhzad, O.C., 2017. Targeted nanotherapeutics encapsulating liver x receptor agonist gw3965 enhance antiatherogenic effects without adverse effects on hepatic Lipid metabolism in Ldlr−/− mice. Adv. Healthc. Mater. 6, 170031.

Zanotti, I., Poti, F., Favari, E., Steffensen, K.R., Gustafsson, J.A., Bernini, F., 2006. Pitavastatin effect on ATP binding cassette A1-mediated lipid efflux from macrophages: evidence for liver X receptor (LXR)-dependent and LXR-independent mechanisms of activation by cAMP. J. Pharmacol. Exp. Ther. 317, 395–401.

Zhang, Y., Zanotti, I., Reilly, M.P., Glick, J.M., Rothblat, G.H., Rader, D.J., 2003. Overexpression of apolipoprotein A-I promotes reverse transport of cholesterol from macrophages to feces in vivo. Circulation 108, 661–663.